Proceedings of the ASME 2010 3rd Joint US-European Fluids Engineering Summer Meeting and
8th International Conference on Nanochannels, Microchannels, and Minichannels
FEDSM-ICNMM2010
August 1-5, 2010, Montreal, Canada

FEDSM-ICNMM2010-30239

NUMERICAL SIMULATION OF A MINI-CHANNEL THREE-WAY CATALYTIC CONVERTER

M.H. Akbari
Assistant Professor

R. Roohi
M.Sc. Student

S.A. Asaee
M.Sc. Student

Faculty of Mechanical Engineering, Shiraz University, Shiraz 71348-51154, Iran

ABSTRACT

A three-dimensional model is developed to simulate the behavior of a single-channel three-way catalytic converter. The flow regime is assumed to be steady and laminar, and the channel walls are considered as isothermal.

A multi-step, global heterogeneous reaction mechanism with 16 reactions and 11 species is used in this investigation to enhance the accuracy of the results. The chemical reactions are assumed to occur only on the reactor walls. The developed model is validated against available experimental data for stoichiometric operating conditions.

The effect of the feed temperature on the conversion efficiency of the main pollutant components is studied. The light-off temperature for the stoichiometric A/F is found to be about 530 K for CO, NO and UHC, and 425 K for H_2 conversion. The model is also applied to predict the effect of reactor length and inlet mixture space velocity on the conversion efficiency at two different temperatures. By using the same kinetics a well-stirred, unsteady model is also developed to identify the sensitivity of the multi-step kinetic mechanism to the mixture composition. The effect of mole fraction variation of each species on the conversion of other mixture components is investigated.

1. INTRODUCTION

The environmental pollution crisis has become one of the main concerns of today's society. Automotive emissions contain many components that contribute to air pollution. The three main harmful components in the engine exhaust gases are unburned hydrocarbons (UHC), carbon monoxide (CO) and nitrogen oxides (NOx). A typical aftertreatment device that is used to reduce all of these pollutants is a three-way catalytic converter (TWC). TWCs consist of a honeycomb structured monolith encased in a metal can which is designed to distribute the flow uniformly through all the monolith channels. Each channel of the monolith is narrow and long and thus the flow can be assumed laminar and fully developed. The distribution of the catalyst material over the channel walls is done through a thin coating layer called the washcoat.

The optimum design of a catalytic converter includes tuning many physical and chemical channel characteristics such as length, porosity, cross section area and metal coverage of the catalyst which make the optimization process a complex procedure [1,2].

Due to the complexity, time consumption and high cost of obtaining experimental results, numerical modeling offers an efficient alternative to obtain the necessary data to simulate the performance of a three-way catalytic converter. In a review work Depcik et al. [3] present the history of the numerical modeling with the assumption of one-dimensionality. The main physical and chemical phenomena which exist inside a TWC are explained thoroughly in this article.

The simulation of the whole catalytic convertor with its multiple channels packed together is the opposite point of the single channel modeling. Hence, there are two conventional approaches to model a TWC reactor. First one is to consider the complete TWC as a channel with the assumption of porous material inside it. The porosity of the channel is calculated based on the void volume of each channel and the thickness of the walls. In the next approach a number of channels with the original geometry are simulated by considering the heat transfer inside the solid monolith structure. This approach is computationally expensive so only a few number of channels are supposed to represent the behavior of the whole TWC. However some authors present new and efficient models to simulate the TWC with its maximum complexities, such as, detailed surface reactions, considering a stack of channels and the effect of multi-dimensionality [4].

Several researchers have concentrated their study on the transport phenomena inside the monolithic converters. The accuracy of the used correlations for the simulation of heat and mass transport in a one-dimensional TWC modeling has a significant effect on the obtained results. It is obvious that 3D modeling does not include this defect and therefore is more reliable.

Santos and Costa [5] examined experimentally the influence of the substrate geometrical and physical parameters on the pollutant removal for several vehicle operating conditions. Several experimental variables were probed, including the outlet gas mixture composition, the temperature at the inlet, outlet and various locations within the substrate of the catalysts. The experimental data revealed that at low space velocities, the ceramic substrate has a better performance in conversion of HC and CO than metallic substrate. Lower thermal conductivity of ceramic than metallic substrate facilitates local ignition and causes the above phenomena.

The same authors in another numerical study [6] use a 1D model to examine the influence of turbulent monolith structures and controlled washcoat structures on TWC conversions. Turbulent monolith structures enhance the channel transport properties and therefore improve the conversion efficiency. They conclude that the net effect of optimizing the transport properties of the washcoat structure has deeper impacts on the TWC conversions than improving the monolith channel structure.

Both the channel transport properties and the kinetic scheme are important parameters for obtaining acceptable results. In general, the HC conversion for small space velocities is kinetically controlled, while for high space velocities it is mass transfer limited; both limitations are less pronounced for the CO conversion and insignificant for the NOx conversion.

The kinetics presented in the literature has a wide variety from a single global reaction to very detailed kinetics. A large number of complex reactions may occur in an exhaust stream that contains O_2, H_2, H_2O and CO_2 as well as CO, HC and NO. Most of the developed kinetic models are based on the rate data obtained for simplified feed streams and single-component fresh catalysts. Thus, they are not adequate for describing three-way catalytic activity under real-world conditions. Therefore it is necessary to conduct a nearly detailed kinetic study over modern TWCs under realistic feed stream conditions.

In the literature there are several works which focus on the presentation of a detailed reaction kinetic model to predict the activity of the commercial three-way catalyst. The vast majority of the kinetic models reported in the literature have been developed based on the Langmuir–Hinshelwood type rate equations [7,8,9]. Most of the TWC researchers use the proposed rate expressions of Voltz et al. [10], and Subramamian and Varma [11] as the main structure of their own simulation; but it should be noted that both of the proposed kinetics are empirical and the range of their validity must be considered.

Kwon et al. [12] presented a detailed kinetic model to predict all possible reactions occurring over a commercial TWC converter. The obtained kinetic can be used to predict the conversion of three major pollutants, including CO, C_3H_6 and NO, as well as formation of NH_3 and N_2O, the secondary air pollutants. The presented kinetic scheme has the capability of tuning the frequency factors for application in the case of aged catalytic converters.

Another recent kinetic model was developed by Kim et al. [2]. This kinetic model contains 10 reactions and 9 species. Three major branches of reactions in a three way catalytic converter which are CO, unburned hydrocarbons (UHC) and NO oxidation are considered accompanied by the water–gas shift and steam reforming reactions. Three different routes for NO reduction are considered in the proposed kinetic, while removal of the major part of NO in the mixture is done through the reaction with the CO.

Investigation of the influence of individual reactions on the conversion efficiency of a TWC has been the main field of interest for some researchers. Hoebink et al. [13] developed a numerical model to explore the effect of CO, H_2, and C_3H_6 on the conversion of NO based on the elementary step kinetics. The presented model applied to predict the pollutant light-off temperature. The obtained results have a good agreement with the available experimental data. H_2 is the most oxygen consumer in the first part of the channel and so has an unpleasant contribution in the NO removal, since without the existence of O_2; NO removal should be achieved through reactions with CO and hydrocarbons which are slower than the oxidation reaction.

In the present work, a three-dimensional model of a single channel catalytic converter is developed. In order to improve the simulation of the washcoat surface treatment, a multi-step reaction kinetics with 16 reactions and 11 species is used. The kinetics used in the present study is based on the semi-experimental rate expression given by Holder et al. [14], and shall be discussed in detail later. The channel walls are assumed to be isothermal, and that the reactions occur only on the wall surfaces. The efficiency of the converter against some input parameters is studied. These parameters include the temperature of the engine exhaust gases for the stoichiometric and lean fuel/air ratios, the gas space velocity and the channel length.

In order to solve the non-linear coupled governing equations, a finite volume method using the SIMPLE algorithm for pressure–velocity linkage is applied. The numerical results are validated against available experimental data.

A transient, one-dimensional and homogeneous model is also developed to investigate the influence of engine exhaust species on the conversion efficiency of different species and to figure out the sensitivity of the reactions. In this model the effect of the variation of mole fraction of each species on the reaction rates and conversion of the pollutants is examined.

2. NUMERICAL MODEL

2.1. Model Geometry

The inside domain of the three-way catalytic converter is simulated as a single narrow channel with a square cross section. The simulated channel is a typical representation of each channel in the whole TWC stack of channels. A schematic configuration of the considered geometry and its dimensions for the baseline modeling are shown in Fig. 1.

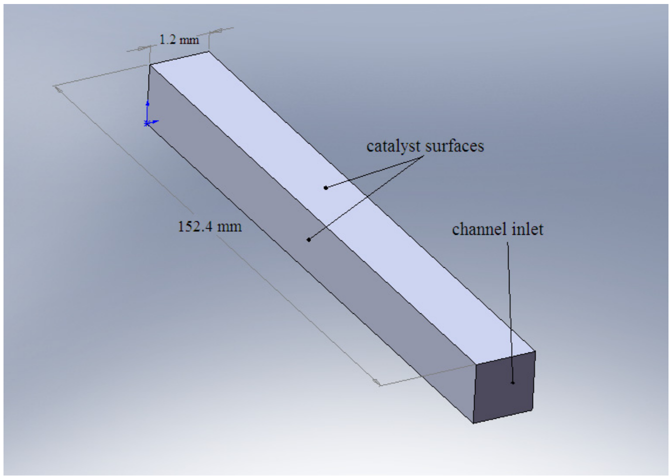

Fig. 1. Schematics and dimensions of TWC channel.

2.2. Model Assumptions and Boundary Conditions

Under the assumption of negligible heat loss to the surroundings and a uniform distribution of the conserved quantities across the inlet face of the monolith, identical boundary conditions prevail for each channel of the monolith and so a single channel may represent the conditions of the entire monolith. Considering fully developed thermal boundary layer, the isothermal boundary condition characterizes the channel wall thermal behavior. The flow regime is assumed to be steady, laminar and incompressible. The gas mixture is treated as an ideal gas with variable properties based on the local composition. The reactions are assumed to be heterogeneous occurring on the channel walls. The input data for the simulation of the converter and the composition of the engine exhaust mixture for two different F/A ratios are listed in Tables 1 and 2, respectively.

Table 1. Input data for the baseline TWC simulation.

Parameter	**Value**	
Space velocity	1.8×10^{6}	h^{-1}
Inlet temperature	525	K
Substrate length	0.1524	m
Side length	1.2	mm
Inlet pressure	101.13	kPa

Table 2. Inlet mole fraction of species.

Species	Mole fraction	
	Stoichiometric F/A (baseline condition)	Lean F/A
CO	6.875×10^{-3}	1.0×10^{-3}
O_2	5.25×10^{-3}	3.75×10^{-2}
CO_2	0.1	0.1
CH_4	1.0×10^{-6}	1.0×10^{-6}
H_2O	0.1	0.1
C_3H_6	4.5×10^{-4}	3.0×10^{-4}
H_2	2.1×10^{-3}	5.0×10^{-5}
NO	3.0×10^{-3}	1.0×10^{-3}
C_3H_8	1.125×10^{-4}	7.5×10^{-4}
N_2O	5.0×10^{-5}	4.0×10^{-5}
N_2	0.782	0.759

2.3. Governing Equations

Using the multi-dimensional form of the governing equations and a detailed kinetics scheme to simulate the flow field and composition of the mixture inside the domain made the modeling computationally expensive. Governing equations include the conservation of mass, momentum, energy and chemical species. Using a rectangular channel, the conservation equations are stated in a Cartesian coordinate system.

The continuum equation for a 3D steady-state flow is given by Eq. (1).

$$\nabla.\left(\rho\vec{V}\right)=0 \tag{1}$$

The Navier-Stokes equation, given below, represents the conservation of momentum for the given conditions.

$$\vec{V}.\nabla\left(\rho\,\vec{V}\right)=-\nabla p+\nabla\cdot\left(\mu\nabla\vec{V}\right) \tag{2}$$

The mass balance for the i^{th} species is given by Eq. (3), with the molar production rate given by Eq. (4) in which ξ is the stoichiometric coefficient of the i^{th} species in the j^{th} reaction.

$$\nabla.\left(\rho\vec{V}\,Y_i\right)=\nabla.\left(D_{eff,i}\,\rho\nabla Y_i\right)+\omega_i MW_i \tag{3}$$

$$\omega_i=\sum_{j=1}^{16}\left(\xi_{ij}\,R_j\right) \tag{4}$$

The conservation of energy is given by Eq. (5) below.

$$\nabla.\left(\rho\,c_p\vec{V}\,T\right)=\nabla.\left(k\nabla T\right)+\sum_{i=1}^{16}\left(\Delta H_i\,R_i\right) \tag{5}$$

Since the chemical reactions occur only on the channel walls, the source terms in Eqs. (3) and (5) are assigned to zero for computations inside the domain while their original values are applied to the calculations at the reactor walls.

Fluid density is computed from the ideal gas equation for a multi-component mixture. The effective mass diffusion coefficient is computed from the following equation,

$$D_{eff,i} = \frac{1-\chi_i}{\sum_{j\neq i}^{\forall j} \frac{\chi_j}{D_{ij}}} \tag{6}$$

where D_{ij} is the binary diffusion coefficient for the species pair *i* and *j*. The constant pressure specific heat, dynamic viscosity and thermal conductivity of the gas mixture are computed based on the local composition of the mixture.

2.4. Solution Method

In order to solve the non-linear, coupled governing equations, a computational fluid dynamics (CFD) code was developed based on the finite volume method using the SIMPLE algorithm for the coupling of pressure and velocity domains. A power-law and a central difference scheme are applied to linearize the convective and diffusive terms, respectively. The algebraic system of equations is solved using the Jacobian point-to-point iteration method, except for pressure correction equation which is solved by exploitation of the Gauss-Seidel iteration method.

To save computational time and avoiding the occurrence of solution divergence, first the governing equations are solved without considering the chemical reactions and property changes for a number of iterations and then the surface reactions take into account. Duo to the stiff nature of the chemical reaction rate equations, small under-relaxation factors are selected and are gradually increased up to 0.99. This will promote stability of the numerical calculations, while securing the accuracy of the numerical results. The effect of grid quantity on the results was also examined and the optimum number of grid points for this case was found to be 150×14×14. The computational time per simulation on a 2.66 GHz Pentium 4 CPU is about 12 hours.

3. CHEMICAL KINETICS

3.1. Chemical Reaction Kinetics Model

In order to consider the major branches involved in pollutant removal from the engine exhaust gases, a semi-empirical, multi-step global reaction mechanism developed by Holder et al. [14] is used. The "three-way catalyst" is Pd/Rh-based with Al_2O_3 support, and 1.7 mg/cm^3 precious metal loading. This mechanism has the original form of the Langmuir–Hinshelwood–Hougen–Watson type and was tuned to simulate fresh and aged catalyst. This mechanism contains 16 reactions and 11 species which are listed in Table 3.

The unburned hydrocarbons consist of C_3H_6 and C_3H_8 which are used to model fast and slow oxidation of UHCs. Although CH_4 is also accounted in the kinetic scheme, its mole fraction is about three orders of magnitude lower than other unburned hydrocarbons.

Table 3. List of reaction equations.

No.	reaction
1	$CO + 0.5O_2 \rightarrow CO_2$
2	$H_2 + 0.5O_2 \rightarrow H_2O$
3	$C_3H_8 + 5O_2 \rightarrow 3CO_2 + 4H_2O$
4	$C_3H_6 + 4.5O_2 \rightarrow 3CO_2 + 3H_2O$
5	$CH_4 + 2O_2 \rightarrow CO_2 + 2H_2O$
6	$CO + H_2O \rightarrow CO_2 + H_2$
7	$C_3H_8 + 3H_2O \rightarrow 3CO + 7H_2$
8	$C_3H_6 + 3H_2O \rightarrow 3CO + 6H_2$
9	$CH_4 + H_2O \rightarrow CO + 3H_2$
10	$CO + NO \rightarrow CO_2 + 0.5N_2$
11	$H_2 + NO \rightarrow H_2O + 0.5N_2$
12	$C_3H_6 + 9NO \rightarrow 3H_2O + 3CO_2 + 4.5N_2$
13	$H_2 + 2NO \rightarrow H_2O + N_2O$
14	$N_2O + H_2 \rightarrow H_2O + N_2$
15	$CO + 2NO \rightarrow CO_2 + N_2O$
16	$N_2O + CO \rightarrow CO_2 + N_2$

Table 4. List of reaction enthalpies and rate expressions.

No.	Rate expression	ΔH_r
1	$\omega_1 = \frac{k_1 X_{CO} X_{O_2}}{F_1}$	−282.85
2	$\omega_2 = \frac{k_2 X_{H_2} X_{O_2}}{F_1}$	−241.70
3	$\omega_3 = \frac{k_3 X_{HC_s} X_{O_2}}{F_3}$	−2042.97
4	$\omega_4 = \frac{k_4 X_{HC_f} X_{O_2}}{F_1}$	−1925.47
5	$\omega_5 = \frac{k_5 X_{CH_4} X_{O_2}}{F_1}$	−801.87
6	$\omega_6 = \frac{k_6 X_{CO} X_{H_2O}}{F_2}$	−41.15
7	$\omega_7 = \frac{k_7 X_{HC_s} X_{H_2O}}{F_2}$	497.48
8	$\omega_8 = \frac{k_8 X_{HC_f} X_{H_2O}}{F_2}$	373.28
9	$\omega_9 = \frac{k_9 X_{CH_4} X_{H_2O}}{F_2}$	206.08
10	$\omega_{10} = \frac{k_{10} X_{CO} X_{NO}}{F_2}$	−373.25
11	$\omega_{11} = \frac{k_{11} X_{H_2} X_{NO}}{F_2}$	−332.10
12	$\omega_{12} = \frac{k_{12} X_{HC_f} X_{NO}}{F_2}$	−2739.1
13	$\omega_{13} = \frac{k_{13} X_{H_2} X_{NO}}{F_2}$	−340.49
14	$\omega_{14} = \frac{k_{14} X_{H_2} X_{N_2O}}{F_2}$	−323.71
15	$\omega_{15} = \frac{k_{15} X_{CO} X_{NO}}{F_2}$	−381.64
16	$\omega_{16} = \frac{k_{16} X_{CO} X_{N_2O}}{F_2}$	−364.86

All reactions can be categorized in three main routes. Reactions 1-5 are basically oxidization reactions that are all exothermic. Steam reforming and the water-gas shift reactions are considered in the second category to simulate the HC and H_2 conversion behavior (reactions 6-9). The last part of this mechanism scheme considers the reduction of NO. Reactions 10-16 represent the two possible pathways in NO removal which are through N_2O and CO.

The reaction enthalpies and rate expressions are listed in Table 4. The inhibition terms of the reaction rate expressions are listed below:

$$k = \exp(A')\exp(-E/RT_s) \tag{7}$$

$$F_1(X,T_s) = T_s(1 + K_{a,1}X_{CO}^{0.2} + K_{a,2}X_{HC_f}^{0.7} + K_{a,3}X_{NO}^{0.7})^2 \tag{8}$$

$$F_2(X,T_s) = T_s(1 + K_{a,4}X_{CO} + K_{a,5}X_{HC_f} + K_{a,6}X_{NO}^{0.7})^2 \tag{9}$$

$$F_3(X,T_s) = T_s(1 + K_{a,1}X_{CO}^{0.2} + K_{a,2}X_{HC_f}^{0.7} + K_{a,3}X_{NO}^{0.7})^2 \times (1 + K_{a.7}X_{O_2}) \tag{10}$$

The kinetic parameter set of the reaction rate constants and inhibition terms are given in Tables 5 and 6.

Table 5. Reaction rate constants.

No.	A'	E **(kJ/mol)**
1	35.60	105.00
2	36.00	85.00
3	36.60	112.00
4	35.30	105.00
5	28.00	121.00
6	20.61	67.44
7	27.70	136.00
8	29.90	116.00
9	26.00	136.00
10	28.60	80.00
11	25.28	71.00
12	24.00	80.00
13	29.80	71.35
14	31.00	80.00
15	27.20	80.00
16	25.80	68.79

Table 6. Reaction rate constants for inhibition terms.

No.	A'	E **(kJ/mol)**
1	2.00	-12.75
2	6.80	-3.00
3	4.50	-9.90
4	5.77	-12.75
5	6.80	-3.00
6	4.50	-9.90
7	11.00	0.00

3.2. Kinetics Sensitivity

Investigation of the sensitivity of a detailed kinetics to its components is an essential part in the modeling of chemical reactions which should be performed to have a better understanding of the kinetic scheme behavior. Thus, in addition to the main model presented for the simulation of a TWC, a homogenous (well-stirred) and unsteady model is also developed to analyze the behavior of the used kinetics as a function of different inlet mixture components. In reality the reactions happen at active sites of the reactor walls. It is obvious that the mixture composition varies along the channel and is not the same as at the inlet. Therefore, the assumption of a homogenous model for the TWC channel might not be true; but the presented model in this part is only applied to explore the sensitivity of the total kinetic to species mole fractions and to make a better understanding of the role of each reaction in the pollutants removal.

The geometry of the reactor and the homogenous mole fraction is selected according to the baseline simulation. The previous discussed kinetics is used to compute the variation of mixture species with time. The duration of the reaction is selected in consistency with the baseline space velocity. At each step the initial mole fraction of a single mixture component is varied while the other mixture components' initial values are held constant at their baseline value. Due to the nature of chemical rate equations the set of the governing equations construct a nonlinear and stiff system of ordinary differential equations. This system of equations is solved by employing an implicit Runge-Kutta formula with a trapezoidal rule step at first stage and a backward second order differentiation formula for the next stage.

In Figs. 2 and 3 the effect of variation of some inlet components mole fraction on the TWC conversion efficiency is shown. The abscissa is the mole fraction of the variable species relative to its magnitude at the baseline condition, and the ordinate is variation of species conversion relative to the obtained conversion in the baseline simulation.

In Fig. 2 the influence of variation of the three main pollutants (CO, C_3H_6 and NO) on the TWC conversion is exposed. In Fig. 2(a) the effect of variation of CO inlet mole fraction is shown. With more CO in the feed mixture conversion of all the displayed species has a decreasing trend with steeper gradient near zero mole fractions of CO. The CO variation consequence is more obvious in the cases of N_2O and C_3H_8 which their conversions grow about 5 times of their original values as the CO mole fraction becomes one tenth.

Fig. 2(b) demonstrates the influence of C_3H_6 on the obtained efficiencies. This behavior is to some extent similar but weaker than the CO effect which was discussed previously. By doubling the C_3H_6 the conversion is reduced about 20% for the other pollutants.

As presented in Fig. 2(c), NO variation has two different effects on the mixture components. First by increasing the amount of NO in the mixture the removal of CO improves, which is due to the increase of N_2O mole fraction in the mixture. Thus the N_2O branch of CO conversion becomes more active. The next effect is decreasing the conversion of other hydrocarbon components. The influence of doubling NO mole fraction is improving the CO and N_2O conversion about 10% and 50%, respectively, and reducing the conversion of hydrocarbons by about 20% compared to their original values.

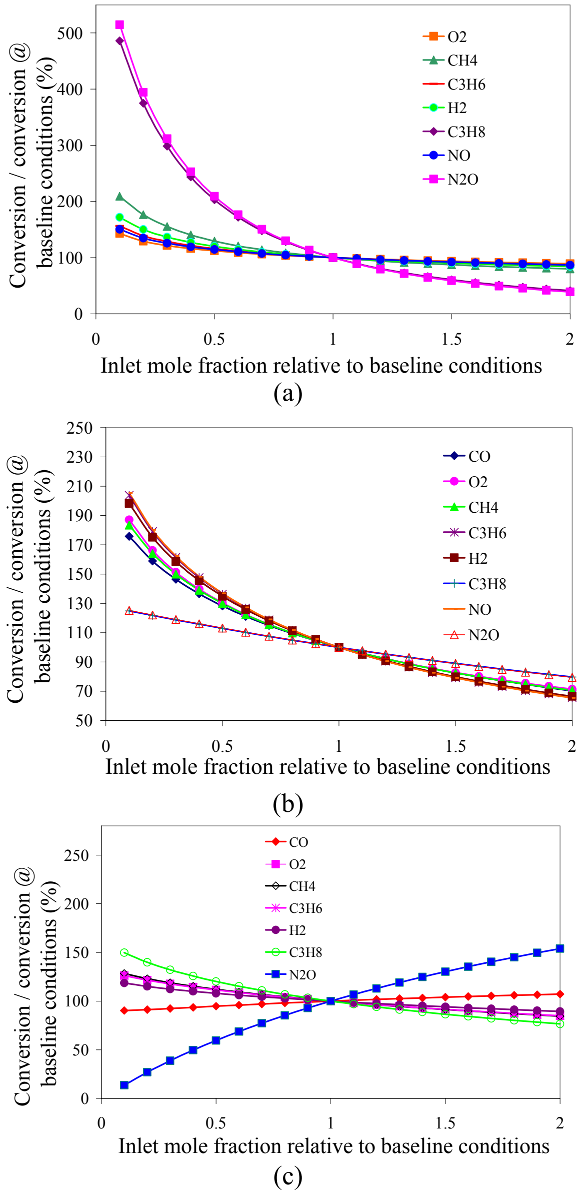

(a)

(b)

(c)

Fig. 2. Effect of inlet mole fractions on conversion (well-stirred model): (a) CO, (b) C_3H_6 and (c) NO.

Fig. 3 represents the effect of other involving species on the behavior of the well-stirred model. The effect of O_2 variations is shown in Fig. 3(a). As expected the conversion efficiency of almost all pollutants are improved with an increase in O_2 mole fraction which is due to the high rate of oxidization reactions. With the exception of NO and N_2O, the conversion of all species increase and for some species such as C_3H_6 and H_2 becomes almost twice with doubling the O_2 inlet mole fraction. This behavior is beneficial in the secondary injection of O_2 in TWCs, especially for rich F/A ratios.

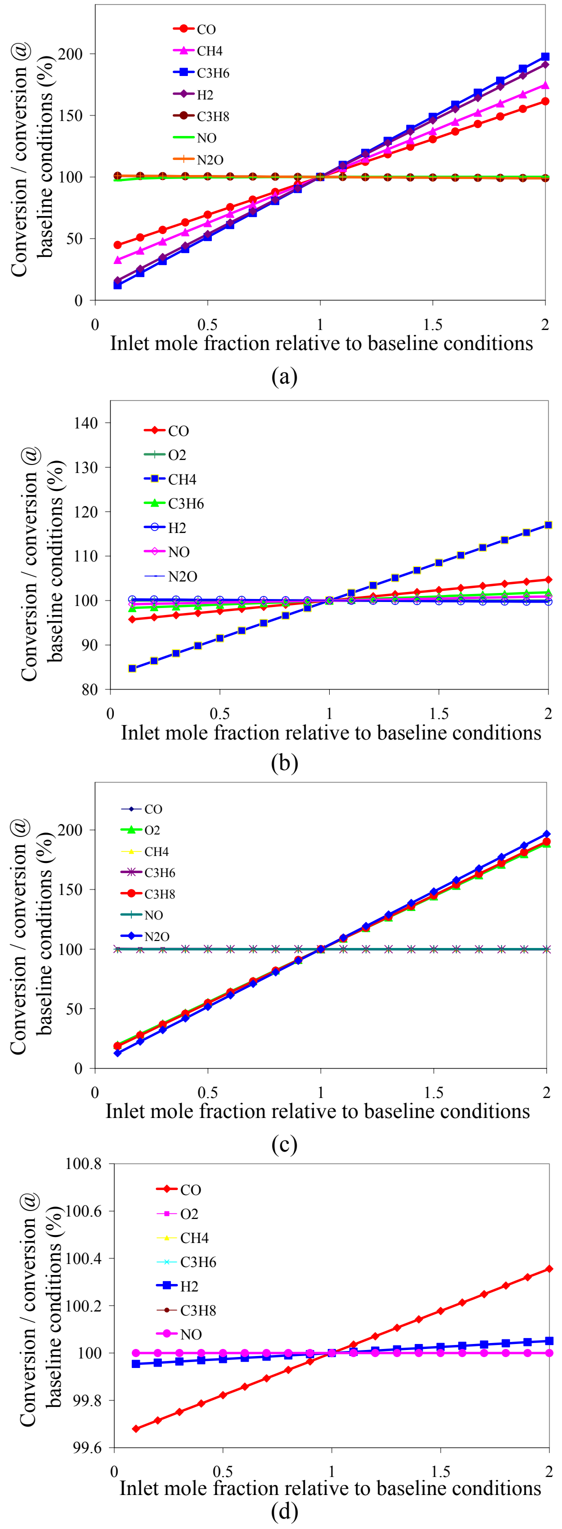

(a)

(b)

(c)

(d)

Fig. 3. Effect of inlet mole fractions on conversion (well-stirred model): (a) O_2, (b) H_2O, (c) H_2 and (d) N_2O.

Fig. 3(b) shows the effect of adding or removing H_2O from the mixture. Except for CH_4 of which there is not a significant amount in the mixture, the influence of variation of H_2O is seen in the improving of conversions by less than 5%. This trend is also obtained for CO_2 variation which has almost no influence on the conversion efficiency of pollutants (not shown). The neutral role of CO_2 and H_2O in the composition of the TWC mixture is also reported by other investigators; see, for example, [6].

As it is obvious from Fig. 3(c) increasing H_2 in the inlet mixture can improve the conversion of C_3H_8 and cause more consumption of O_2 mixture content, however it has nearly no effect on other pollutants' removal. These behaviors are the results of fast reaction of H_2 and O_2, and the importance of H_2 and C_3H_6 reaction path on the removal of this unburned hydrocarbon, respectively.

Shown in Fig. 3(d), N_2O has little positive effect on CO conversion and almost no effect on the other species. The small magnitude of N_2O mole fraction in the original mixture is the reason for its neutral behavior on other species conversion efficiency. However, this conclusion should not be confused with the major effect of N_2O reaction route in the removal of pollutants, especially CO.

4. RESULTS AND DISCUSSION

The developed model is applied to simulate the behavior of a TWC. The obtained results are validated against available experimental data and the predicted conversion efficiency trend matches the previous works. A parametric study is conducted to explore the effect of geometrical variations of the channel, such as cross section area and channel length at two different temperatures. In addition, the effect of space velocity and the feed temperature (for lean and stoichiometric F/A ratio) on removal of the pollutants is investigated.

4.1. Baseline Simulation

For the baseline simulation a one-channel catalytic converter with square cross section is simulated. These dimensions are selected according to the Holder et al. [14] geometric configuration and are listed in Table. 1. For assuring the convergence of the numerical simulation the convergence condition for the average relative errors are set to 10^{-5}.

The calculation results indicate that fully developed flow is reached at a distance 10 times the hydraulic diameter of the channel, and that the peak value of the axial velocity component increases to twice the value of the inlet velocity. Both of these results are compatible with theoretical and experimental expectations for this three-dimensional channel flow.

Plotted in Fig.4 are the relative mole fraction of different mixture components along the channel for two different temperatures; these are the fractions relative to the inlet values.

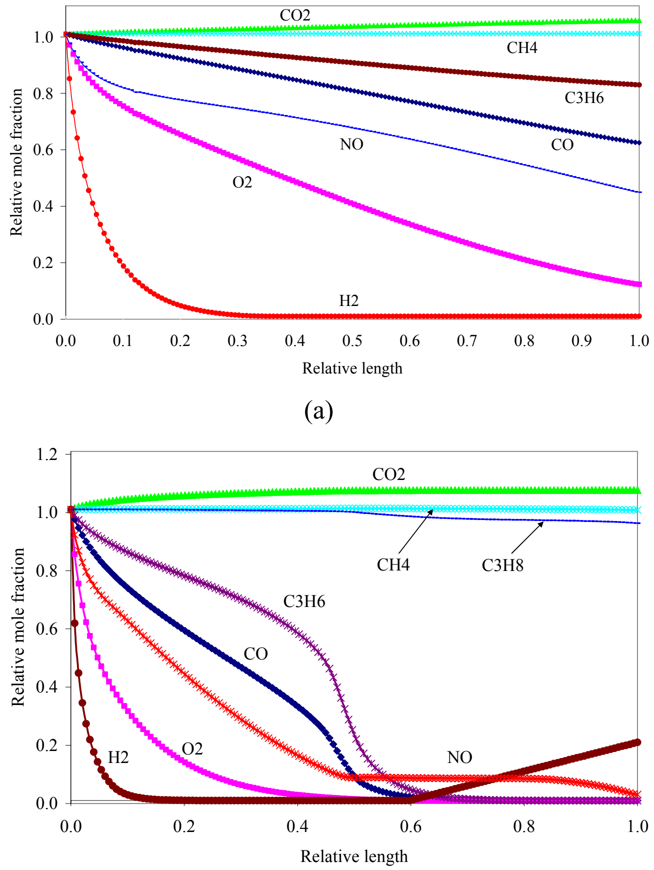

(a)

(b)

Fig. 4. Species mole fraction variation along the channel related to inlet value: (a) T_{in}=525 K and (b) T_{in}=575 K.

In Fig. 4(a) the feed temperature is selected equal to the baseline value. It is observed that the consumption of C_3H_6, CO and CH_4 are uniform and linear through the channel. Complete removal of H_2 occurs at nearly a quarter of the length channel. It is also observed that NO reduction is reduced after that region, which is due to the removal of H_2. This behavior is a result of a decrease in the rate of reactions 11 and 13 because of the removal of H_2. In Fig. 4(b) the same results are shown for an elevated temperature (575 K). The variation of H_2 relative mole fraction in this graph is remarkable. At about 10% of the channel length the whole amount of H_2 is converted and so in the same region the variation of other species such as CO, NO, C_3H_6 and O_2 is steeper due to their high rated reactions with hydrogen. Between the 10% to about 50% of the channel length there is a reducing trend in this graph similar to the first 10% length of the channel but with decreased gradients.

The conversion of O_2 is completed within the first half of the channel length and with a high rate. In this region the complete conversion of almost all dominant pollutants occur, except NO and C_3H_8. In the second half of the channel length the mole fraction of H_2 is increased. The production of hydrogen in this part can be described by considering reactions

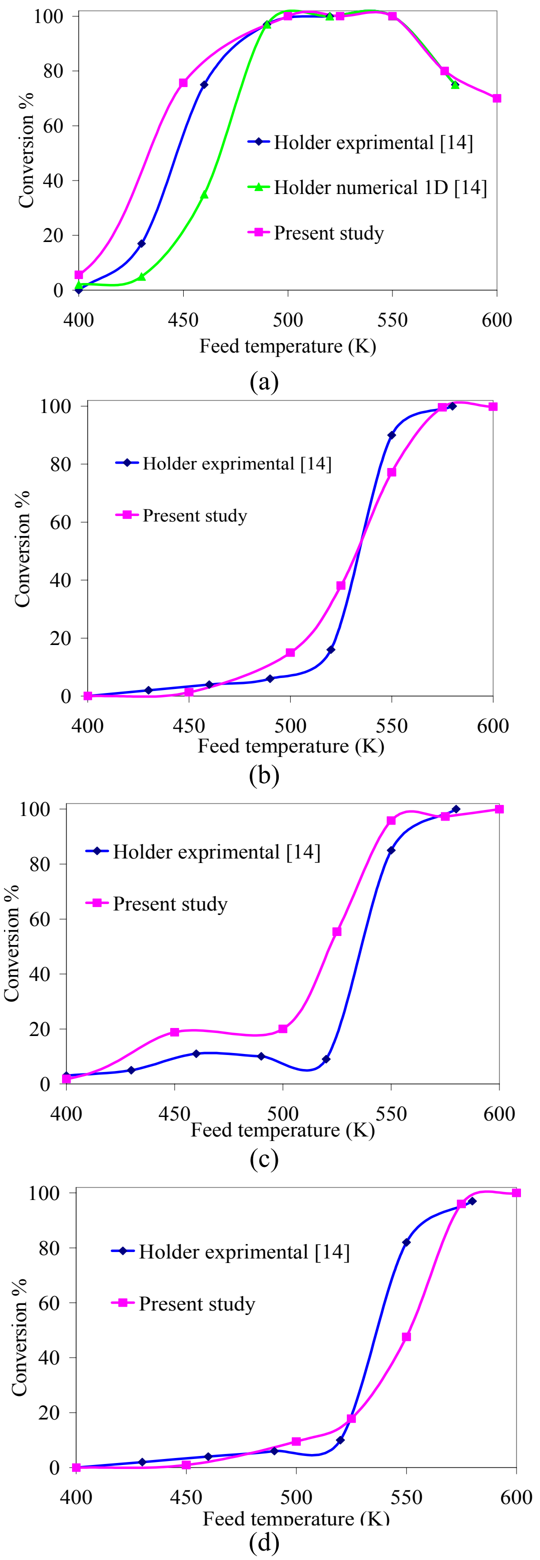

Fig. 5. Effect of feed temperature on conversion and validation against experimental results for stoichiometric A/F: (a) H_2, (b) CO, (c) NO and (d) C_3H_6.

7 and 9. The rates of these reactions are nearly zero and so the production of H_2 by them is negligible. In the first half of the channel length the amount of H_2 that is produced by these reaction is rapidly consumed by other fast H_2 consuming reactions (reactions 2, 11 and 13), but in the second half where the rate of H_2 consuming reactions are negligible, the small amount of produced H_2 is retained.

4.2. Validation

In Fig. 5 the conversion efficiencies of main pollutants and H_2 are plotted versus the feed gas temperature for the stoichiometric fuel/air ratio.

Comparison of the numerical results with the experimental data measured under the same conditions [14] shows a good agreement between them. In Fig. 5(a) moreover, the predicted conversion of H_2 is compared by a previous 1D model and a better matching of the current 3D model conversion efficiency with the experimental data is seen. The light-off temperature, that is, the temperature for 50% conversion efficiency, is to some extent lower in the case of H_2 compared to the other pollutant species. Also reduction of H_2 conversion efficiency at high temperatures is well predicted by the numerical model. Reduction of oxygen content in the mixture at high temperatures (reaction no. 2) and activation of the water-gas shift and steam reforming reactions (reactions no. 6-9) at those temperatures are the reasons for this behavior.

The light-off temperatures obtained for H_2, CO, NO and C_3H_6 are about 425, 530, 520 and 550 K, respectively.

4.3. Parametric Study

In this section, the influence of the channel length and inlet gas space velocity on TWC performance is investigated. These parametric studies are conducted in two different feed temperatures, so a more precise analysis can be performed. Lastly, the effect of feed temperature on the TWC conversion characteristics is examined at two different F/A ratios. It is noted here that the effects of the channel length and space velocity have been investigated separately (and not in a combined form in terms of the residence time) since the heterogeneous reactions are not volumetric, rather, they occur on the channel reactor walls. In such a case, the space velocity of the feed gas is not expected to have the same effect on the overall conversion as that of the channel length.

4.3.1. Effects of Channel Length

The effect of variation of the channel length is an important parameter in the design of a TWC which should be considered. The ranges of selected channel length for simulation are between 120-152.4 mm. For the results shown in Fig. 6(a) the feed temperature and the other boundary conditions are selected according to the baseline simulation.

As it is expected the conversion is improved while the channel length is increased. As the channel is extended the residence time inside the reactor is increased and so the reactions have more time to occur which improves the performance of the TWC.

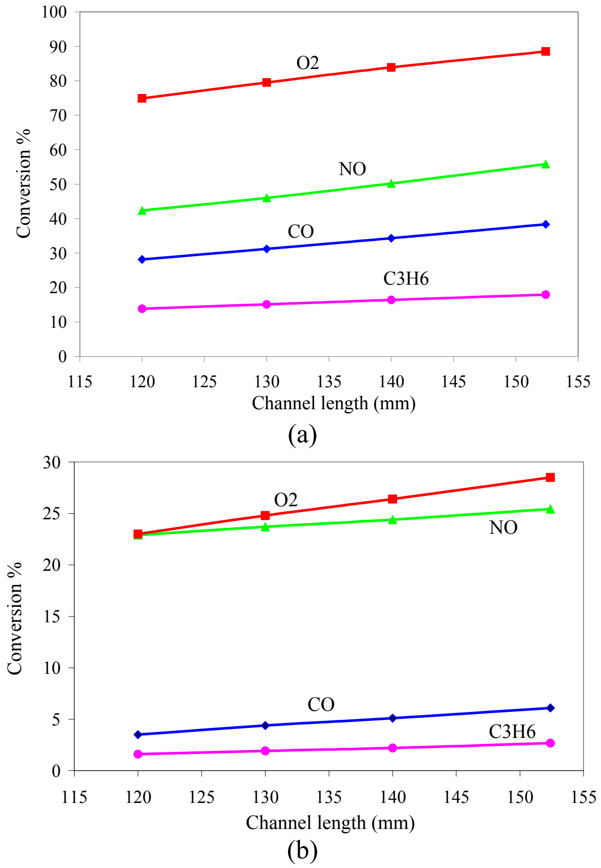

Fig. 6. Effect of channel length on conversion: (a) T_{in}=525 K and (b) T_{in}=475 K.

In the reactors there is always a length which longer than that no significant improving in the conversion can be occurred. This length at which complete conversion happens does not reach for two considered feed temperatures. Longer channel lengths haven't enough interest in this article because there is a typical range for channel lengths which are common in TWCs. The conversion is improved about 10 % for all species as the length of the channel is increased from 120 to 152.4 mm.

The next graph in this part (Fig. 6(b)) shows the same behavior for the reduced feed temperature. The obtained conversions are linearly increased with length. The improvement in conversion for this condition is only about 3 % for the conversion of pollutants.

4.3.2. Effects of Space Velocity

The variation of TWC conversion efficiency as a function gas space velocity is another parameter which is studied here. In Fig. 7(a) the feed temperature is set to 525K and the results revealed that as the space velocity is decreased the conversion efficiency improved.

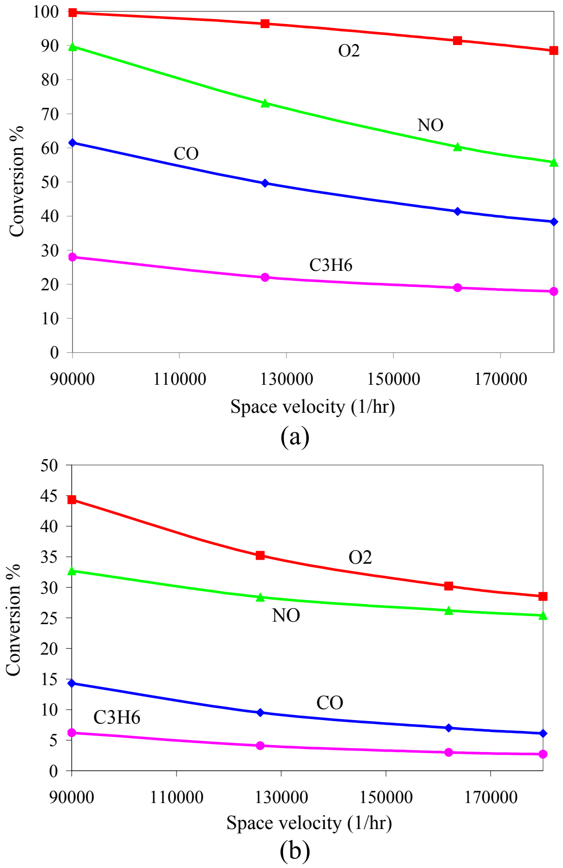

Fig. 7. Effect of gas space velocity on conversion: (a) T_{in}=525 K and (b) T_{in}=475 K.

By reducing the space velocity to half, the conversion of CO, NO and C_3H_6 recovered about 23, 34 and 10%, respectively. The space velocity has almost the same influence on the channel chemical behavior as the channel length. This is due to the effect of both of them on the residence time of the reactions in three-way catalytic converter.

In Fig. 7(b) the same study is conducted for a reduced inlet temperature (475 K). The improvement in the conversion efficiency by reducing the space velocity to its half value is about 8, 7 and 3.5% for CO, NO and C_3H_6 respectively. The amount of conversion increasing with space velocity is more in the case of higher temperatures. Comparison between Fig. 7(a) and 7(b) shows that at the same space velocity the conversion is improved as a function of the feed temperature.

The pressure drop along the channel is investigated in Fig. 8 as a function of gas space velocity and channel side length at three different temperatures.

As shown in this figure increasing the space velocity causes an increase of the pressure drop along the channel. At elevated temperatures the pressure drop is increased further. Thus, the lowest viable gas space velocity has the benefits of both minimizing the pressure drop and maximizing the pollutants conversion.

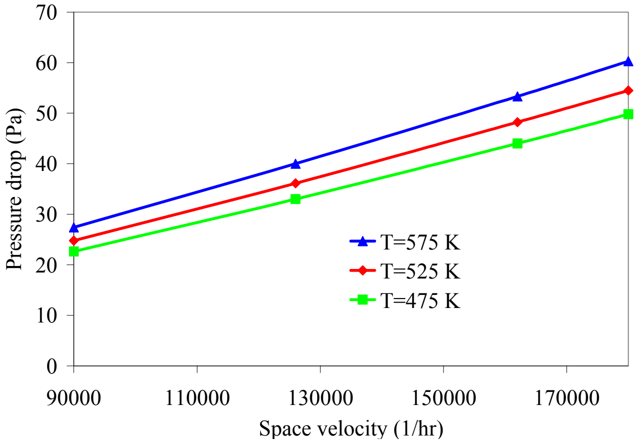

Fig. 8. Effect of gas space velocity and side length on the channel pressure drop for different feed temperatures.

4.3.3. Effects of Inline Temperature

The effect of feed temperature for the lean engine F/A ratio operating condition is shown in Fig. 9. The predicted light-off temperature for CO and C_3H_6 is about 475 K which is lower than the same results for the stoichiometric F/A ratio. The conversion behavior of NO is displayed in part (b) of this graph. Its maximum conversion occurs at the feed temperature of 500 K at a value of 10%.

5. CONCLUSIONS

A three-dimensional, single channel model with a multi-step heterogeneous kinetic scheme is developed to simulate the conversion efficiency of a three-way catalytic converter. Validation is performed against experimental data which shows acceptable accuracy in the prediction of the conversion efficiency of a TWC for all three including pollutants besides hydrogen for stoichiometric F/A ratio. The obtained light-off temperature for all the species is obtained at about 530 K, except for H_2 which is found at 425 K duo to its fast reactions. As well, this model is utilized in the case of lean F/A ratio and the effect of feed temperature in this case is investigated.

The effect of cell density on the conversion efficiency is studied and the results show that decreasing the side length to 0.8 mm for baseline temperature and to about 0.7 mm for the reduced feed temperature of 475 K can cause a complete removal of the pollutants. Furthermore the effect of variation of length and space velocity is examined. These calculations are performed at both temperatures of 475 K and 525 K. As the residence time of the reactions is increased, which is done by increasing the channel length or decreasing the space velocity, the conversion is improved at either temperatures, although it is less obvious in lower temperatures.

To capture a better understanding of the role of individual species in the used kinetics a homogenous (well-stirred) and unsteady model is developed to specify the effect of variation of each component mole fraction in the conversion efficiency.

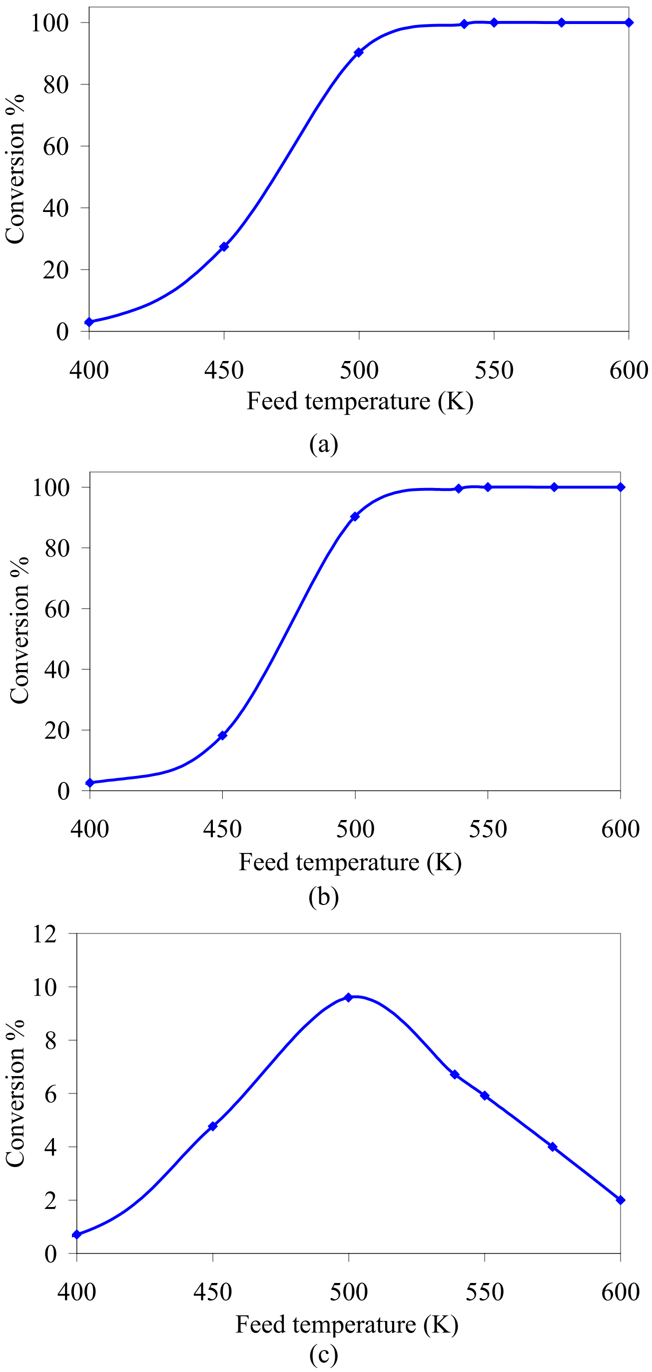

Fig. 9. Effect of feed temperature on conversion of species for lean A/F: (a) CO, (b) C_3H_6 and (c) NO.

The results revealed that as the amount of CO and C_3H_6 in the mixture is increased the conversion of other species is reduced. O_2 injection in the inlet composition can improve the conversion of all the pollutants. NO variation has two opposite consequences in conversion of pollutants. Some species almost have no influence on the conversion efficiency of presented well-stirred model, such as H_2O, CO_2, CH_4 and N_2O.

6. NOMENCLATURE

A'	kinetic parameter
c_p	constant pressure specific heat *(kJ/kg.K)*
D	binary diffusion coefficient *(m^2/s)*
E	activation energy *(kJ/kmol)*
F	inhibition term
ΔH_r	reaction enthalpy *(kJ/kmol)*
k	thermal conductivity *(W/m.K)* or reaction rate coefficient
MW	molecular weight *(kg/kmol)*
P	pressure *(Pa)*
R	total reaction rate *($kmol/m^3.s$)*
R_u	universal gas constant *(J/kmol.K)*
T	temperature *(K)*
$\vec{V}$	velocity vector *(m/s)*
Y	species mass fraction

Greek symbols

ξ	stoichiometry coefficient
μ	kinematic viscosity *($N.s/m^2$)*
ω	species reaction rate *($kmol/m^3.s$)*
ρ	density *(kg/m^3)*
χ	species mole fraction

Sub or superscripts

eff	effective
i	i^{th} species or reaction
j	j^{th} species or reaction
s	channel surface
mix	gas mixture

7. REFERENCES

[1] Jeong SA, Kim WS. A study on the optimal monolith combination for improving flow uniformity and warm-up performance of an auto-catalyst. Chem. Eng. Process. 2003;42, pp. 879-895.

[2] Kim YD, Jeong SJ, Kim WS. Optimal design of axial noble metal distribution for improving dual monolithic catalytic converter performance. Chem. Eng. Sci. 2009;64, pp. 1373-1383.

[3] Depcik C, Assanis D. One-dimensional automotive catalyst modeling. Prog. Energy Comb. Sci. 2005;31, pp. 308-369.

[4] Kumar A, Mazumder S. Toward simulation of full-scale monolithic catalytic converters with complex heterogeneous chemistry. Comp. Chem. Eng. 2010;34, pp. 135-145.

[5] Santos H, Costa M. Modeling transport phenomena and chemical reactions in automotive three-way catalytic converters. Chem. Eng. J. 2009;148, pp. 173-183.

[6] Santos H, Costa M. Evaluation of the conversion efficiency of ceramic and metallic three way catalytic converters. Energy Convers. Manage. 2008;49, pp. 291-300.

[7] Manuel I, Thomas C, Colas H, Matthess N, Djéga-Mariadassou G. A new approach in the kinetic modelling of three-way catalytic reactions. Top Catal. 2004;30/31, pp. 311-317.

[8] Dubien C, Schweich D, Mabilon G, Martin B, Prigent M. Three-way catalytic converter modeling: fast- and slow-oxidizing hydrocarbons, inhibiting species, and steam-reforming reaction. Chem. Eng. Sci. 1998;53, pp. 471-481.

[9] Ma LP, Bart HJ, Ning P, Zhang A, Wu G, Zengzang Z. Kinetic study of three-way catalyst of automotive exhaust gas: modeling and application. Chem. Eng. J. 2009;155, pp. 241-247.

[10] Voltz SE, Morgan CR, Liederman D, Jacob SM. Kinetic study of carbon monoxide and propylene oxidation on platinum catalysts. Ind. Eng. Chem. Prod. Res. Dev. 1973; 12, pp. 294-301.

[11] Subramanlam B, Varma A. Reaction kinetics on a commercial three-way catalyst: the CO-NO-O_2-H_2O system. Ind. Eng. Chem. Prod. Res. Dev. 1985;24, pp. 512-516.

[12] Kwon HJ, Baik JH, Kwon YT, Nam IS, Oh SH. Detailed reaction kinetics over commercial three-way catalysts. Chem. Eng. Sci. 2007;62, pp. 5042-5047.

[13] Hoebink JHBJ, van Gemert RA, van den Tillaart JAA, Marin GB. Competing reactions in three-way catalytic converters: modeling of the NOx conversion maximum in the light-off curves under net oxidising conditions. Chem. Eng. Sci. 2000;55, pp. 1573-1581.

[14] Holder R, Bollig M, Anderson DR, Hochmuth JK. A discussion on transport phenomena and three-way kinetics of monolithic converters. Chem. Eng. Sci. 2006;61, pp. 8010-8027.